Journal of Power Sources 195 (2010) 6232–6238

Contents lists available at ScienceDirect

Journal of Power Sources

journal homepage: www.elsevier.com/locate/jpowsour

A dye-sensitized photo-supercapacitor based on PProDOT-Et_2 thick films

Chih-Yu Hsu [a], Hsin-Wei Chen [a], Kun-Mu Lee [b], Chih-Wei Hu [c], Kuo-Chuan Ho [a,c,*]

[a] Department of Chemical Engineering, National Taiwan University, Taipei 10617, Taiwan
[b] Photovoltaics Technology Center, Industrial Technology Research Institute, Hsinchu 31040, Taiwan
[c] Institute of Polymer Science and Engineering, National Taiwan University, Taipei 10617, Taiwan

ARTICLE INFO

Article history:
Received 8 October 2009
Received in revised form
17 December 2009
Accepted 18 December 2009
Available online 13 January 2010

Keywords:
Charge transfer
Dye-sensitized solar cell (DSSC)
Photocapacitor
PProDOT-Et_2
Supercapacitor

ABSTRACT

A photo-rechargeable supercapacitor (photo-supercapacitor, or PSC) is studied using a N3-dye adsorbed TiO_2 photoelectrode and PProDOT-Et_2 poly(3,3-diethyl-3,4-dihydro-2H-thieno-[3,4-b][1,4]dioxepine) polymer films as supercapacitor materials for electron storage. The PSC device, comprising a dye-sensitized solar cell (DSSC) and a supercapacitor (SC), can store the photo-to-electric energy. The PProDOT-Et_2 films are potentiostatically electropolymerized to form thick films (*ca.* 0.5 mm) with a specific capacitance of *ca.* 6.5 F cm^{-2}. A symmetrical (p/p) supercapacitor, with PProDOT-Et_2 coated on both electrodes, is also characterized before fabricating the three-electrode PSC. The PSC is tested under light illumination of 100 mW cm^{-2}, and attaining a photocharged voltage of 0.75 V and a discharged energy density of 21.3 μWh cm^{-2}.

1. Introduction

Solar-energy conversion and electric energy storage are becoming key techniques towards issues on energy crisis and sustainable use. For the solar-energy conversion, as mostly by the form of solar cell, dye-sensitized solar cells (DSSCs) with nanocrystalline TiO_2, dye molecules, and electrolytes are recently developed for light harvesting [1–3]. The step for solar cells from silicon-based solar cell [4] to DSSCs is mainly because of the possible low production cost and the designability of dye molecule for expected higher energy conversion efficiency comparing with inorganic metal systems. However, it still requires another technique in conjunction with solar cells to store the generated electric energy. There are designs developed as a combined function of solar-energy conversion and electric energy storage in a single device structure to store the light energy *in situ* [5–7]. These efforts are mainly designed by using a photoactive electrode in combination with redox-active materials to store the energy in the form of electrochemical potential. There are also some designs using similar concept with the properties of secondary battery for the storage role [8,9]. Furthermore, Miyasaka's group [10,11] combined a DSSC with a capacitor for electric storage since the rapid response to photocurrent and long lifetime comparing with redox-active materials. The integration of solar-to-electric conversion and storage is current research interest for *in situ* storage and the exploration of better storage materials for future development.

In the developments of secondary batteries, conducting polymer-based supercapacitors [12–16] are a recently growing topic due to similar reasons of the development of DSSCs in solar cells, the low-cost availability and designability of monomers. Besides, their fast redox switching, low toxicity, good conductivity, and mechanically flexible applicability reflect an intensive application as good electrode materials for supercapacitor [15,16] comparing with transition metal oxides. The commonly investigated conducting polymers, such as polypyrrole, polyaniline, and poly(3,4-ethylenedioxythiophene) (PEDOT) show promising usage for their excellent specific capacitance [17]. In particular, PEDOT (structure shown in Fig. 1) has been demonstrated an electrode specific capacitance (C_E) approaching 5 F cm^{-2} which is higher than all other reported materials, although its mass specific capacitance (C_M) is relatively small [14]. The electrode's specific capacitance can be considered as an evaluated parameter for capacitor materials that reflects the practically utilized capacity over a unit geometric area of the electrode [18]. Rather than the mass specific electrode, i.e. the capacitance over a unit mass of the materials on electrodes, the evaluation of electrode specific capacitance should be suitable to present the electric storage efficiency for composite device application, such as photocapacitor. On the other hand, PEDOT belongs to a derivative of poly(3,4-alkylenedioxythiophene)s (PXDOTs), and these derivatives have

* Corresponding author at: Department of Chemical Engineering, National Taiwan University, No. 1, Sec. 4, Roosevelt Rd., Taipei 10617, Taiwan. Tel.: +886 2 2366 0739; fax: +886 2 2362 3040.
E-mail address: kcho@ntu.edu.tw (K.-C. Ho).

0378-7753/$ – see front matter © 2010 Elsevier B.V. All rights reserved.
doi:10.1016/j.jpowsour.2009.12.099

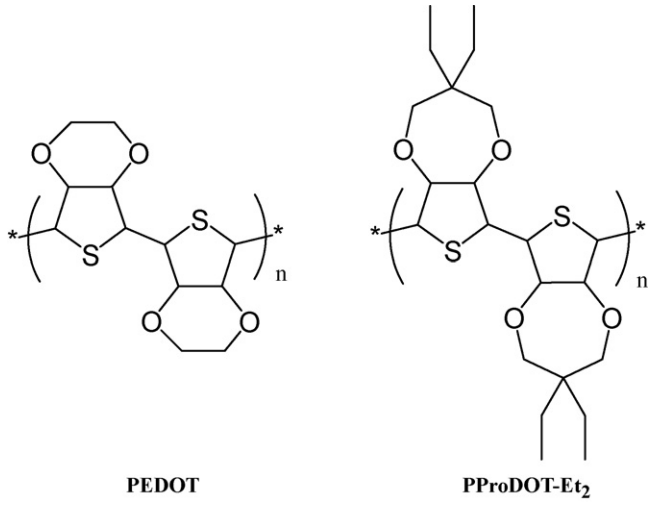

Fig. 1. Structure of PEDOT and PProDOT-Et_2.

been greatly investigated by Reynolds' group [19–21] and employed in many optoelectronic fields, including supercapacitors [22,23]. In these derivatives, poly(3,3-diethyl-3,4-dihydro-2H-thieno-[3,4-b][1,4]dioxepine) (PProDOT-Et_2) (structure shown in Fig. 1) was reported to exhibit enhanced redox properties and stability [24], which may be resulted from space created by the diethyl substituents for facile ion movement during redox process. As discussed before, the redox reversibility and charge–discharge stability are important for conducting polymers to play as supercapacitor materials. Therefore, PProDOT-Et_2 can be served as a good candidate for supercapacitor electrode materials, despite there are no reports about its application on supercapacitors.

In our earlier study [25], we demonstrated a so-called photoelectrochromic device using a PProDOT-Et_2 thin film and a photoactive TiO_2 layer to capture the light-generated electrons and exhibited color change. Such concept is also a kind of combined function of solar-energy conversion and electric energy storage in a single device structure. However, because of the existence of redox couple, the storage efficiency is restrained. Here, we report a photocharging type supercapacitor (namely, photo-supercapacitor, or PSC) using a N3-dye (bis(isothiocyanato)ruthenium(II)-bis-2,2′-bipyridine-4,4′-dicarboxylic acid) adsorbed TiO_2 photoelectrode and PProDOT-Et_2 polymer thick films as supercapacitor materials. The performance of PProDOT-Et_2 used in symmetrical type supercapacitor was explored and compared with that of PEDOT. The PSC device, comprising a DSSC and a supercapacitor, which efficiently stores the solar-to-electric energy storage, was studied. We employed a new combination of DSSC and polymer-based supercapacitor with low-cost availability for high voltage and energy output.

2. Experimental

2.1. Chemicals

The monomer, 3,4-ethylenedioxythiophene (EDOT) and 3,4-(2′,2′-diethylpropylene)-dioxythiophene (ProDOT-Et_2), was purchased from Aldrich and so were $LiClO_4$, LiI and poly(ethyleneglycol) (PEG) (MW 20,000), 4-*tertiary*-butyl pyridine (TBP) obtained from Merck. The above chemicals were used as received. Acetonitrile (ACN), 3-methoxypropionitrile (MPN) and *tertiary*-butanol were also obtained from Merck and water molecules were removed by molecular sieves (4 Å). Titanium(IV) tetraisopropoxide (>98%) was purchased from Acros and used as received. N3 dye was obtained from Solaronix (Aubonne, Switzerland).

2.2. Preparation of polymer thick films and supercapacitors

The PEDOT and PProDOT-Et_2 thick films were electropolymerized from the bath solution composed of 0.2 M monomer and 0.1 M $LiClO_4$ in ACN using a three-electrode system with a potentiostat (Autolab, Eco Chemie, PGSTAT 30). By applying a constant potential of 1.0 V (*vs.* Ag/Ag^+) onto a Pt disc of 0.1 cm diameter or a Pt-sputtered (*ca.* 100 nm thick) glass substrate of 0.25 cm^2 active area, the passed charge was kept at 0.05 or 60 C cm^{-2}, respectively. Two of the prepared electrodes of *ca.* 0.5 mm film thickness (60 C cm^{-2} case) were then put face-to-face to assemble the symmetrical (p/p) supercapacitor separated by an electrolyte of 0.5 M $LiClO_4$ in MPN.

2.3. Preparation of photoactive TiO_2 electrodes and assembly of PSC

The TiO_2 nanoparticle preparation and electrode fabrication were carried out according to the literature [26] except after autoclave treatment, where the solution was concentrated to 13 wt% and PEG was added to prevent film from cracking during drying. The TiO_2 paste was coated onto FTO glass using a glass rod, and then sintered at 500 °C for 30 min. An active area of 0.25 cm^2 was selected from the sintered TiO_2 electrode and immersed in a 3×10^{-4} M solution of N3 dye containing ACN and *tertiary*-butanol (in a volume ratio of 1:1) overnight.

The PSC cell was assembled with the photoactive electrode and the Pt-sputtered glass at one of the outside surface of the supercapacitor separated by the electrolyte composed of 0.5 M LiI/0.05 M I_2/0.5 M TBP in CH_3CN. The device structure is shown in Fig. 2, which can be realized as three-electrode type configuration that the DSSC and supercapacitor sharing a common Pt electrode.

2.4. Apparatus and characterization

The polymer film electrodes were characterized using cyclic voltammetry (CV) technique by a three-electrode system. The polymer film electrodes were scanned in 0.5 M $LiClO_4$/MPN solution for different scan rates. The impedance spectra of the electrodes were recorded at 0.4 V in the frequency ranging from 0.01 to 10 kHz with sinusoidal signal (single sine) and an ac amplitude (ΔE_{ac}) of 10 mV. The charge–discharge behavior of the supercapacitor was tested by using galvanostatic method.

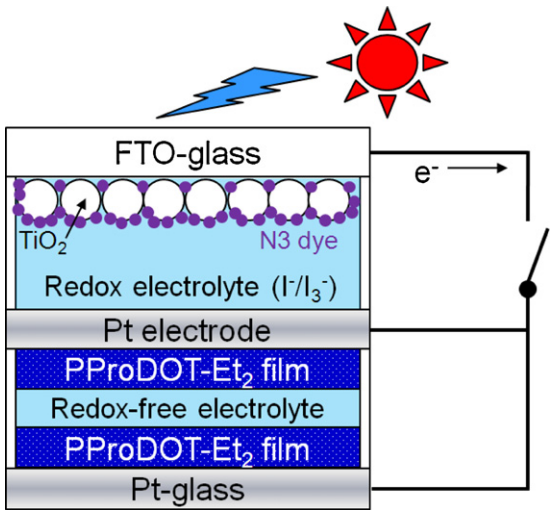

Fig. 2. Device configuration of the three-electrode photo-supercapacitor (PSC), which consists of a dye-sensitized solar cell (DSSC) and a symmetrical PProDOT-Et_2 polymer-based supercapacitor (SC). The DSSC and SC shares a common Pt electrode.

For the photocharging process of PSC, it was placed under a solar simulator (Pecell Technologies, PEC-L11) under AM 1.5 simulated light illumination. The device was short-circuited by connecting those three electrodes (see Fig. 2) for the photo-generated electrons flowing from the photoactive electrode to the supercapacitor. The two outer electrodes were connected together to set as working electrodes and the inner electrode was set as counter electrode. The voltage difference of the PSC was generated due to the working function of the DSSC [1–3], which also determines the maximum charging voltage of the supercapacitor. The electrons were therefore stored at the conducting polymer phases by positive and negative double-layer charging. For the discharging process of PSC, the external circuit was switched that made only the two electrodes from the supercapacitor as positive and negative electrodes, respectively, were connected to the potentiostat. A galvanostatic discharge of 2 mA cm^{-2} was employed between the two electrodes of supercapacitor. The PSC can be tested repeatedly under the above charge–discharge cycles.

3. Results and discussion

3.1. The electrochemical properties of PEDOT and PProDOT-Et_2 films

In order to realize the electrochemical properties of PProDOT-Et_2 as the electrode material for supercapacitor, more-studied PEDOT [14,17] was used and compared with PProDOT-Et_2. The cyclic voltammograms (CVs) of the PEDOT and PProDOT-Et_2 modified Pt electrodes were recorded in 0.1 M $LiClO_4$/MPN solution with different scan rates as shown in Fig. 3(a) and (b). It is noticed that the charge capacities of each films here are controlled at lesser 50 mC cm^{-2} to show clearly the redox peak resulted from Faradaic current for characterizing their electrochemical nature. The typical redox reactions for PEDOT and PProDOT-Et_2 can be briefly described below according to the two literatures [24,27]:

$$[(EDOT^{+})_n](nClO_4^{-}) + ne^{-} \leftrightarrow (EDOT)_n + nClO_4^{-} \quad (1)$$

$$[(ProDOT\text{-}Et_2^{+})_n](nClO_4^{-}) + ne^{-} \leftrightarrow (ProDOT\text{-}Et_2)_n + nClO_4^{-} \quad (2)$$

where $(EDOT)_n$ and $(ProDOT\text{-}Et_2)_n$ represent PEDOT and PProDOT-Et_2, respectively. According to Fig. 3(a) and (b), the electrochemical responses of both materials should be similar to those with a surface-confined coatings, because the redox peak currents were linearly proportional to the scan rates as predicted for a diffusionless conducting polymer film. Both CVs show a fast current switching at the end of positive potential scan, indicative of a capacitor behavior. Moreover, it is shown that CV shape of PProDOT-Et_2 is sharper and the redox peaks are more obvious than that of PEDOT, which can be explained from the difference of ring size and substitution [21], as shown in Fig. 1.

The heterogeneous charge transfer rate constant, k_s, of the PEDOT and PProDOT-Et_2 films were calculated from the CVs obtained at different scan rates as reported by Laviron [28] from the data of Fig. 3(a) and (b). The peak potential difference (ΔE_p) should be ≥200 mV for each electron transfer, i.e. the requirement of the calculation, that can be found at a scan rate above 0.3 V s^{-1} in

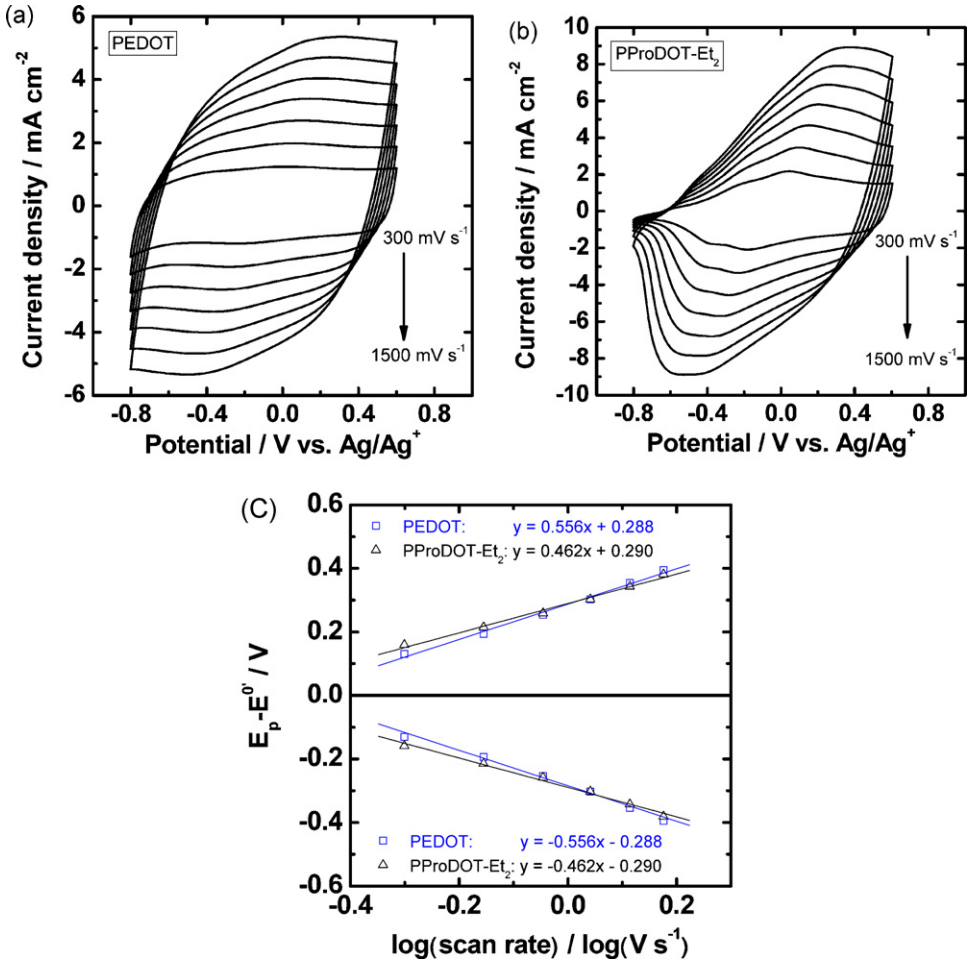

Fig. 3. Cyclic voltammograms of (a) PEDOT and (b) PProDOT-Et_2 thin films (50 mC cm^{-2}) on Pt disc (0.1 cm diameter) in 0.5 M $LiClO_4$/MPN solution at different scan rates of 300, 500, 700, 900, 1100, 1300 and 1500 mV s^{-1}. (c) The corresponding $E_p - E^{0\prime}$ *vs.* log(scan rate).

our cases. Fig. 3(c) shows the plots of the difference between peak potential and the formal potential ($E_p - E^{0\prime}$) *vs.* log υ, for the scan rate (υ) above 0.3 V s^{-1}. It was found that $E_p - E^{0\prime}$ varies linearly with log υ. Under this condition, α (charge transfer coefficient) and k_s were calculated from Eq. (3):

$$\log k_s = \alpha \log(1-\alpha) + (1-\alpha) \log \alpha - \log\left(\frac{RT}{nF\upsilon}\right) - \alpha(1-\alpha)nF\left(\frac{\Delta E_p}{2.3RT}\right) \quad (3)$$

where α was calculated from slopes and using the formulas $-2.3RT/\alpha nF$ (cathodic) or $2.3RT/(1-\alpha)nF$ (anodic), and being found to be 0.11 and 0.13 for PEDOT and PProDOT-Et$_2$, respectively, υ used was 1.1 V s^{-1} and its corresponding ΔE_p was used. Other symbols have their usual meanings. The values of the heterogeneous rate constant, k_s, of PEDOT and PProDOT-Et$_2$ polymer films are found to be 0.61 and 0.49 s^{-1}, respectively. The higher k_s value indicates the higher charge transfer rate for PEDOT than PProDOT-Et$_2$.

3.2. The capacitance behavior of PEDOT and PProDOT-Et$_2$ films

With the understanding of the electrochemical characteristics of PProDOT-Et$_2$ relative to PEDOT, all films were prepared to be thick for exhibiting their capacitance behavior. The CVs of the two materials of 60 C cm^{-2} charge capacity were recorded at a narrower potential range that resembles a rectangle, as shown in Fig. 4. For an ideal capacitor, Faradaic current should not be involved but only the charging current which leads to a rectangular CV shape. From both Fig. 4(a) and (b), the CV shapes were distorted at the higher scan rate of 2 mV s^{-1}, indicating a ohmic resistance of the electron transfer and ionic movement in the polymer film [29]. Such behavior is related to the film thickness and scan rate. Besides, the distortion of PProDOT-Et$_2$ thick film (Fig. 4(b)) at higher scan rate is more obvious than that of PEDOT (Fig. 4(a)) which infers that either the film is thicker or the ohmic resistance is larger for PProDOT-Et$_2$. As discussed earlier, the charge transfer rate constant, k_s, of PEDOT is higher than that of PProDOT-Et$_2$, therefore the resistance is correspondingly larger for PProDOT-Et$_2$. Furthermore, the film thickness can also be explained from the following interpretation of C_E and C_M values.

The specific capacitance is often obtained from plateau of the charging current and the scan rate of the CV curve [30], as shown in Eq. (4):

$$C = \frac{i}{\upsilon} = \frac{i}{\Delta V/\Delta t} \quad (4)$$

where C is the specific capacitance in F, i is the charge/discharge current in A, $\Delta V/\Delta t$ is the scan rate in V s^{-1}. The C_E values for PEDOT and PProDOT-Et$_2$ are approximately 5.24 and 6.52 F cm^{-2}, respectively, calculated using the average current of the middle plateau in Fig. 4. However, the CV technique has been considered dynamic to over-estimate the capacitance due to the extra contribution from Faradaic reaction. Therefore, electrochemical impedance spectroscopy (EIS) is introduced as a steady-state measurement for representing the true capacitance [31]. Fig. 5 shows the EIS results of PEDOT and PProDOT-Et$_2$ thick films measured at 0.4 V. The specific capacitance can be obtained from the reciprocal slope by plotting $-Z''$ *vs.* $(2\pi f)^{-1}$, which is known as low frequency capacitance, as shown in Eq. (5):

$$-Z'' = \frac{1}{C_E}(2\pi f)^{-1} \quad (5)$$

where $-Z''$ is the imaginary impedance value in ohm, and f is the frequency in Hz. From the inset of Fig. 5, the EIS measured specific capacitances of PEDOT and PProDOT-Et$_2$ were calculated and summarized in Table 1. The C_E and C_M values were obtained according to specific capacitance per unit electrode active area and per unit

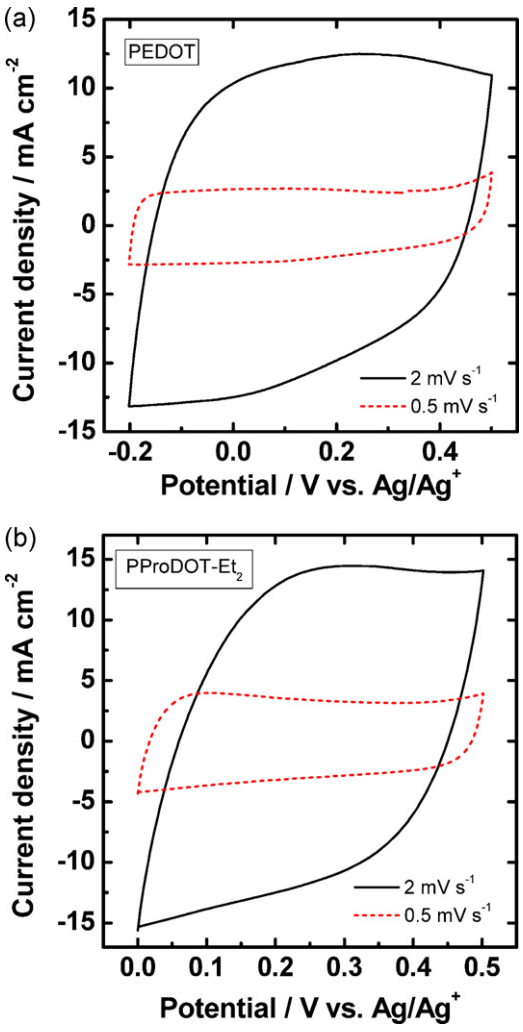

Fig. 4. Cyclic voltammograms of (a) PEDOT and (b) PProDOT-Et$_2$ thick films (60 C cm^{-2}) on Pt disc (0.1 cm diameter) in 0.5 M $LiClO_4$/MPN solution at the scan rate of 2 and 0.5 mV s^{-1}.

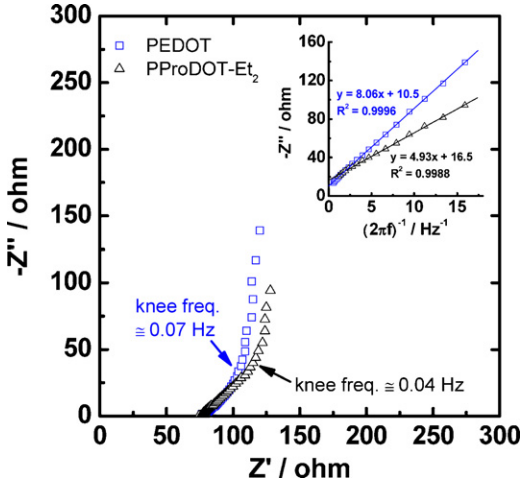

Fig. 5. Complex plane impedance plots of PEDOT and PProDOT-Et$_2$ thick films (60 C cm^{-2}) on Pt disc (0.1 cm diameter) measured at 0.4 V *vs.* Ag/Ag$^+$ in 0.5 M $LiClO_4$/MPN solution. Inset: the corresponding linear relations between Z'' and $1/(2\pi f)$ for the two films.

Table 1
The summary of the mass and electrode specific capacitances of PEDOT and PProDOT-Et_2.

Electrode materials	C_M ($F g^{-1}$)	C_E ($F cm^{-2}$)
PEDOT	164.5	4.09
PProDOT-Et_2	81.9	6.46

weight of the electrode material, respectively. From Table 1, the C_M value of PEDOT is comparable with earlier works [17,32], and it is higher than that of PProDOT-Et_2 because the smaller molar mass of EDOT monomeric unit. While the C_E value of PProDOT-Et_2 is contrarily higher than that of PEDOT, which infers that the electroactive amount on the electrode or the film thickness of PProDOT-Et_2 is greater than PEDOT. The film thickness effect can also be observed from the distortion of CV shape at higher scan rate as discussed previously for Fig. 4. The morphology of PProDOT-Et_2 is more porous resulted from polymer stacking process with its larger ring size and ethyl substitution [24] as shown in Fig. 1. Such an open morphology facilitates the film growing to a thicker film with more electroactive species on the electrode. Therefore, the C_E value of PProDOT-Et_2 can achieve higher performance than that of PEDOT, which is valuable in device application. Besides, the C_E value of *ca.* 6.5 $F cm^{-2}$ also gets beyond the earlier report [14] in which they declared the highest value ever.

From the calculation by CV and EIS, it is also noticed that the over-estimation of PEDOT is higher than PProDOT-Et_2, i.e. 5.24 $F cm^{-2}$ (CV) *vs.* 4.09 $F cm^{-2}$ (EIS) for PEDOT and 6.52 $F cm^{-2}$ (CV) and 6.46 $F cm^{-2}$ (EIS) for PProDOT-Et_2. This is also expected because of the larger k_s value of PEDOT. The faster charge transfer reaction indicates that the Faradaic reaction is facilely arisen. So the scan rate of the CV measurement of PEDOT is recommended to be even lower for true estimation of capacitance. On the other hand, the complex plane plots of Fig. 5 show a deviation from the vertical line at higher frequencies, at which the deviation occurs is called knee frequency [33]. The higher knee frequency indicates a faster charge–discharge speed of the film. Thus, the charge–discharge speed of PEDOT film is higher than that of PProDOT-Et_2, and this phenomenon is also correspond to the k_s values compared earlier. The ratios for knee frequencies and k_s values of PEDOT to PProDOT-Et_2 are also similar and the magnitude of order between knee frequency and k_s values are also about the same, indicating a reliable evaluation of charge transfer speed.

3.3. The performance of the supercapacitor and photo-supercapacitor

Despite PEDOT exhibits slightly better charge–discharge rate, the total accessible capacitance, C_E, of PProDOT-Et_2 is the major concern for the material of the following practical systems. Before testing the photo-supercapacitor (PSC), a symmetrical (p/p) type supercapacitor using PProDOT-Et_2 as the electrode material was fabricated. It is generally classified into three types of conducting polymer-based supercapacitor: a symmetrical system of both p-dopable, an asymmetric system of two different p-dopable, and a symmetrical system of both p- and n-dopable for the electrode materials [12]. While polythiophene derivatives have difficulties of n-doping [34], a symmetrical (p/p) type supercapacitor was attempted. Fig. 6 shows the galvanostatic charge/discharge responses of PProDOT-Et_2 thick films based supercapacitor at the current density of 2 $mA cm^{-2}$ between 0 and 1.0 V for the first 5 cycles. According to the concept of Eq. (4), the C_E value of the supercapacitor can be determined from the applied current and the slope of the discharge curves, which is about 0.48 $F cm^{-2}$. The lower C_E value related to earlier discussion on electrodes is probably due to the electroactive area effect, since the area has an 8

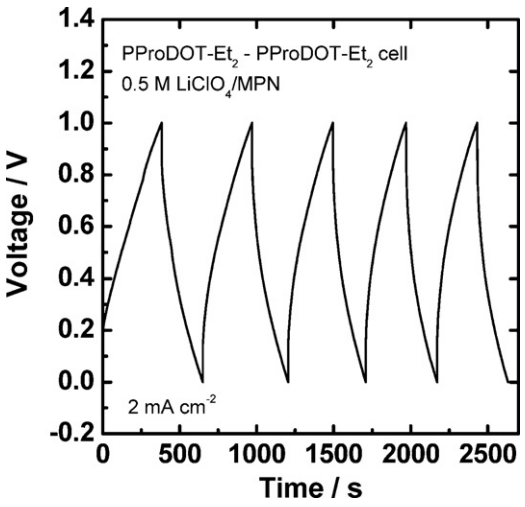

Fig. 6. Galvanostatic charge–discharge curves of supercapacitor at a constant current density of 2.0 $mA cm^{-2}$.

times increment from Pt disc to Pt-sputtered substrate. In order to achieve a practical system, the device should be presented in a certain scale despite a lesser production of capacitance. Such effect is also observed from the charge/discharge efficiency of *ca.* 80%, which is the ratio of discharge time and charge time, for a slightly unsymmetry in Fig. 6. In fact, it can be seen from Fig. 5 that the knee frequency is 0.04 Hz, implying the existence of a rather thick film. The reason that the charge/discharge efficiency is not high for PProDOT-Et_2 has to do with the thicker film we used, which is about 0.5 mm. The thicker the film, the larger the electrical resistance is. This explains a low value of the charge/discharge efficiency. Even so, the C_E value of 0.48 $F cm^{-2}$ is still high compared with other supercapacitor works using PXDOT as electrode materials [23,31,35–37] with around 0.009–0.17 $F cm^{-2}$.

Hereafter, the supercapacitor is combined with a typical dye-sensitized solar cell as a three-electrode configuration to fabricate a PSC. The photocharge/electric discharge process of the PSC is presented in four steps as indicated in Fig. 7, where Fig. 7(a) is the current responses and Fig. 7(b) is the voltage responses of the PSC although they are not *in situ* data. For the first step, the PSC was connected to the potentiostat and placed without light illumination, and there are no current and voltage responses. It implies that the DSSC did not produce dark current since the circuit was already connected. Then, the light turned on to start the photocharge under 100 $mW cm^{-2}$ visible light irradiation. During the photocharge, an anodic photocurrent of *ca.* 7 $mA cm^{-2}$ occurred as shown in Fig. 7(a). This current density, generated from the DSSC part, was comparable with the general magnitude of the DSSC. The anodic current response represents the direction of the electron flowing from the photoactive TiO_2 electrode to the supercapacitor for charging. The corresponding charging voltage as shown in Fig. 7(b) is *ca.* 0.75 V, which is determined from the photovoltage of the DSSC part. The higher the charging voltage for a capacitor, the more energy it can stored. Although the supercapacitor part can definitely allow the cell voltage beyond 0.75 V, this voltage is suitable for the use in electronic devices. Both the current and voltage increased rapidly once the light illumination was switched on, and then each shows stable as a function of charging time. The charging process of the PSC is surely from the light and reliable.

As for the discharge, the light was switched off for the following third step and the charged PSC was also left in the open-circuit condition by disconnecting the switch as shown in Fig. 2. The current was immediately returned to zero (Fig. 7(a)) since no electron is generated. The voltage of the PSC still held at *ca.* 0.75 V with a slight drop (Fig. 7(b)) due to self-discharge. The maintenance of the

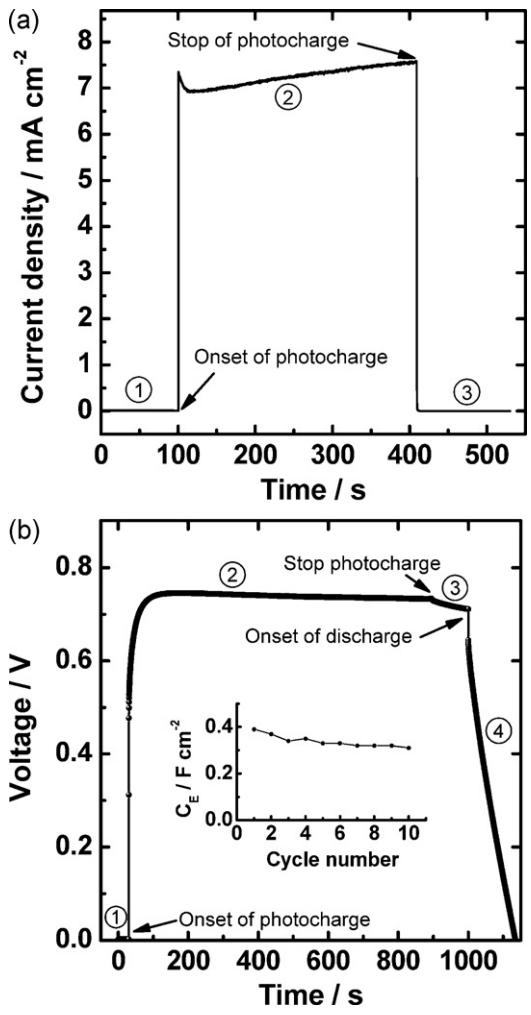

Fig. 7. Changes in (a) the photocurrent density and (b) the cell voltage during photocharging and discharging. The inset in (b) is the discharged C_E value as a function of the cycle number.

cell voltage indicates the success of photocharge. After the third step, discharge of the PSC was carried out by connecting only to the supercapacitor part. The discharge current was set at 2 mA cm^{-2} between the two electrodes of the supercapacitor part. Fig. 7(b) exhibits a constant decreased profile of the voltage with time. The initial small drop at the onset of discharge is resulted from the internal resistance of capacitors [38]. According to this profile, the C_E of the PSC is calculated via Eq. (4) as 0.39 F cm^{-2}. This value is close to the earlier calculated result for the sole supercapacitor of 0.48 F cm^{-2}. So the PSC was photocharged completely by the light illumination. The cycle performance of the PSC was done for another 10 cycles according to the steps stated above. The result is shown in the inset of Fig. 7(b), which indicates the discharged C_E values of the PSC that can be determined quantitatively at the 4th step as a function of the cycle number. The C_E values decreased slightly only in the first few cycles and became relatively stable with *ca.* 80% retention of its original value at the 10th cycle. Since the PSC can be regarded as a combination of a DSSC and a supercapacitor, the cycle performance can be assured with the two existing technologies. Moreover, the energy density (E_d in Wh cm^{-2}) and power density (P_d in W cm^{-2}) of the PSC can also be calculated by the following two equations from the discharge profile in Fig. 7(b):

$$E_d = i \int V\, dt \tag{6}$$

$$P_d = \frac{E_d}{t_d} \tag{7}$$

where t_d is the discharged time in s. The E_d and P_d values per unit electrode area were thus obtained as 22 μWh cm^{-2} and 0.6 mW cm^{-2}. If the 100 mW cm^{-2} light intensity is assumed as the energy source input, the output P_d value of 0.6 mW cm^{-2} indicates an energy storage efficiency of the PSC is equivalent to 0.6%.

4. Conclusions

We proposed a novel photo-supercapacitor (PSC) using PProDOT-Et$_2$ conducting polymer thick film as energy storage material and N3 dye-TiO$_2$ DSSC for the direct storage of sunlight energy. The capacitance properties of first-investigated PProDOT-Et$_2$ were studied with the comparison of PEDOT. PEDOT possesses higher mass specific capacitance (C_M) due to smaller molar mass of monomer. The charge–discharge rate of PEDOT polymer is also better than that of PProDOT-Et$_2$ according to the analysis of CV and EIS measurements. The charge transfer rate constant, k_s, of PEDOT film was obtained as 0.61 s^{-1} which is higher than that of PProDOT-Et$_2$ film of 0.49 s^{-1}. This shows similar result with the knee frequency from EIS. While at thick film status, PProDOT-Et$_2$ possesses higher electrode specific capacitance (C_E) due to its porous nature for film growing. According to the steady-state measurement of capacitance from EIS, the C_E value of PProDOT-Et$_2$ thick film achieved *ca.* 6.5 F cm^{-2} which is chosen for the material of PSC fabrication. The PProDOT-Et$_2$ based supercapacitor and PSC exhibited specific capacitance of *ca.* 0.48 F cm^{-2}, energy density of *ca.* 22 μWh cm^{-2} and power density of *ca.* 0.6 mW cm^{-2}, which is equivalent to an energy storage efficiency of 0.6%. The PSC can provide photocharge voltage of 0.75 V, which is suitable for the use in electronic devices.

Acknowledgements

This work was financially sponsored by a grant from the National Taiwan University. Some of the instruments used in this study were made available through the support of the National Science Council (NSC) of Taiwan.

References

[1] B. O'Regan, M. Grätzel, Nature 353 (1991) 737–740.
[2] M. Grätzel, Nature 414 (2001) 338–344.
[3] Y.C. Hsu, H. Zheng, J.T. Lin, K.C. Ho, Sol. Energy Mater. Sol. Cells 87 (2005) 357–367.
[4] D.M. Chapin, C.S. Fuller, G.L. Pearson, J. Appl. Phys. 25 (1954) 676–677.
[5] S. Licht, G. Hodes, R. Tenne, J. Manassen, Nature 326 (1987) 863–864.
[6] A. Hauch, A. Georg, U.O. Krasovec, B. Orel, J. Electrochem. Soc. 149 (2002) A1208–A1211.
[7] H. Nagai, H. Segawa, Chem. Commun. (2004) 974–975.
[8] T. Kanbara, K. Takada, Y. Yamamura, S. Kondo, Solid State Ionics 40–41 (1990) 955–958.
[9] X. Zou, N. Maesako, T. Nomiyama, Y. Horie, T. Miyazaki, Sol. Energy Mater. Sol. Cells 62 (2000) 133–142.
[10] T. Miyasaka, T.N. Murakami, Appl. Phys. Lett. 85 (2004) 3932–3934.
[11] T.N. Murakami, N. Kawashima, T. Miyasaka, Chem. Commun. (2005) 3346–3348.
[12] A. Rudge, J. Davey, I. Raistrick, S. Gottesfeld, J.P. Ferraris, J. Power Sources 47 (1994) 89–107.
[13] P. Sivaraman, V.R. Hande, V.S. Mishra, Ch. Srinivasa Rao, A.B. Samui, J. Power Sources 124 (2003) 351–354.
[14] G.A. Snook, C. Peng, D.J. Fray, G.Z. Chen, Electrochem. Commun. 9 (2007) 83–88.
[15] C. Arbizzani, M. Mastragostino, F. Soavi, J. Power Sources 100 (2001) 164–170.
[16] A. Malinauskas, J. Malinauskienė, A. Ramanavičius, Nanotechnology 16 (2005) R51–R62.
[17] K. Lota, V. Khomenko, E. Fracowiak, J. Phys. Chem. Solids 65 (2004) 295–301.
[18] M. Wu, G.A. Snook, V. Gupta, M. Shaffer, D.J. Fray, G.Z. Chen, J. Chem. Mater. 14 (2005) 2297–2303.
[19] A. Kumar, D.M. Welsh, M.C. Morvant, F. Piroux, K.A. Abboud, J.R. Reynolds, Chem. Mater. 10 (1998) 896–902.

[20] L. Groenendaal, F. Jonas, D. Freitag, H. Pielartzik, J.R. Reynolds, Adv. Mater. 12 (2000) 481–494.
[21] L. Groenendaal, G. Zotti, P.H. Aubert, S.M. Waybright, J.R. Reynolds, Adv. Mater. 15 (2003) 855–879.
[22] J.D. Stenger-Smith, C.K. Webber, N. Anderson, A.P. Chafin, K. Zong, J.R. Reynolds, J. Electrochem. Soc. 149 (2002) A973–A977.
[23] A.S. Sarac, H.D. Gilsing, A. Gencturk, B. Schulz, Prog. Org. Coat. 60 (2007) 281–286.
[24] C.L. Gaupp, D.M. Welsh, J.R. Reynolds, Macromol. Rapid Commun. 23 (2002) 885–889.
[25] C.Y. Hsu, K.M. Lee, J.H. Huang, K.R. Justin Thomas, J.T. Lin, K.C. Ho, J. Power Sources 185 (2008) 1505–1508.
[26] M.K. Nazeeruddin, R. Humphry-Baker, P. Liska, M. Grätzel, J. Phys. Chem. B 107 (2003) 8981–8987.
[27] T.S. Tung, K.C. Ho, Sol. Energy Mater. Sol. Cells 90 (2006) 521–537.
[28] E. Laviron, J. Electroanal. Chem. 101 (1979) 19–28.
[29] P.H. Aubert, L. Groenendaal, F. Louwet, L. Lutsen, D. Vanderzande, G. Zotti, Synth. Met. 126 (2002) 193–198.
[30] J. Tanguy, N. Mermilliod, M. Hoclet, J. Electrochem. Soc. 134 (1987) 795–802.
[31] J. Bobacka, A. Lewenstam, A. Ivaska, J. Electroanal. Chem. 489 (2000) 17–27.
[32] R. Liu, S.I. Cho, S.B. Lee, Nanotechnology 19 (2008) 215710.
[33] C.M. Niu, E.K. Sichel, R. Hoch, D. Moy, H. Tennent, Appl. Phys. Lett. 70 (1997) 1480–1482.
[34] H.J. Ahonen, J. Lukkari, J. Kankare, Macromolecules 33 (2000) 6787–6793.
[35] V. Noel, H. Randriamahazaka, C. Chevrot, J. Electroanal. Chem. 558 (2003) 41–48.
[36] H. Randriamahazaka, C. Plesse, D. Teyssie, C. Chevrot, Electrochim. Acta 50 (2005) 4222–4229.
[37] A.K.C. Gallegos, M.E. Rincon, J. Power Sources 162 (2006) 743–747.
[38] A. Du Pasquier, I. Plitz, J. Gural, S. Menocal, G. Amatucci, J. Power Sources 113 (2003) 62–71.